ZNO NANOROD-BASED MSM PHOTODECTORS FABRICATED ON FLEXIBLE SUBSTRATES

L. W. Ji[*], C. Z. Wu[*], T. H. Fang[*], C. H. Liu[*], T. H. Meen[*], K. T. Lam[**], J. C. Shen[***]

[*]Institute of Electro-Optical and Materials Science, National Formosa University, Yunlin 632, Taiwan, ROC

[**]Institute of Microelectronics & Department of Electrical Engineering, National Cheng Kung University, Tainan 701, Taiwan, ROC

[***]Department of Automation Engineering, National Formosa University, Yunlin 632, Taiwan, ROC

Introduction

ZnO is a wide direct-gap semiconductor with a large exciton binding energy of 60 meV and bandgap energy of 3.37 eV at room temperature, and it is regarded as a promising photonic material instead of GaN for optoelectronic applications in the ultraviolet (UV) spectral range.[1-4] One-dimensional (1D) materials such as nanowires (NWs), nanobelts and nanorods (NRs) have attracted considerable interest in recent years.[5-6] They present the utmost challenge to semiconductor technology, making possible fascinating novel devices. Among them, 1D ZnO nanostructures have been demonstrated a variety of functional device applications in the past decade, such as light-emitting diodes (LEDs),[7] nanolasers,[8] photodetectors (PDs),[9-11] field-effect transistors (FET), [12, 13] photovoltaic devices,[14] nanogenerators,[15] and chemical sensors,[16] *etc*. There is another growing interest today in flexible electronics such as wearable displays, detectors, and sensors. The flexible polymeric substrate, which has poor thermal endurance and requires all films on it made at low temperatures, is often used for this kind of products[17, 18]. Since ZnO NRs can be prepared by low temperature processes, in contrast with the other wide bandgap materials like GaN and SiC, its related devices on flexible substrates will become important applications in the future.

In this work, we report the fabrication and characterization of a novel metal-semiconductor-metal (MSM) UV photodetectors (PDs) on PET with ZnO NRs. The NR arrays were selectively grown on the gap of interdigitated electrodes by chemical solution method through a novel photolithography process. The traditional ZnO MSM photodetectors with no nanorods have been simultaneously made in comparison with the former. We found the fabricated novel UV photodetectors demonstrated a higher photoresponse and UV-to-visible rejection ratio than the traditional ZnO MSM PDs.

Device design and fabrication

Before the device fabrication, 500-nm-thick ZnO seed layers were deposited onto PET substrates using radio frequency (rf) magnetron sputter deposition technique. 100-nm-thick Ag electrodes were subsequently deposited onto the ZnO film by electron beam evaporation to serve as Schottky contacts while lithography was performed for defining the interdigitated contact pattern. The fingers of the Ag contact electrodes were 150 μm long and 10 μm wide with 10 μm spacing. The active area of the whole device was 150×160 μm^2. Then we employed the photoresists in protecting the electrode patterns by lithography technique. The sample with photoresist-protected interdigitated electrodes was subsequently immersed in the $Zn(NO_3)_2$/ $C_4H_{13}N_3$ (DETA) aqueous solution for 3 hours at 90 ^oC. The fabricated MSM photosensors were removed from the solution, rinsed with distilled water and dried in air. Finally, we removed the photoresists from the interdigitated electrode surface of devices. The schematic structure of ZnO NR MSM PD is shown in figure 1. On the other hand, the traditional MSM PDs with 500-nm-thick ZnO film were fabricated for comparison, where no ZnO NRs can be found.

Experimental results and discussion

X-ray diffraction (XRD), micro-photoluminescence (micro-PL), and high-resolution transmission electron microscopy (HRTEM, JEOL JEM-3010) were then used to characterize the optical and crystallographic properties of the as-grown ZnO NRs. Surface morphologies of the NRs and NR PDs were

characterized by a field-emission scanning electron microscope (FESEM, JEOL JSM-6700F). An HP-4156C semiconductor parameter analyzer was then used to measure current-voltage (*I-V*) characteristics of the fabricated ZnO NR PDs. Spectral responsivity measurements were also performed by TRAIX 180 system with a 300-W xenon arc lamp light source and a standard synchronous detection scheme.

Figure 2(a) shows the XRD and PL results (inset) of the as-grown ZnO NR arrays. The XRD pattern of ZnO nanorods indicates three reflection peaks of hexagonal wurtzite structure, [002], [101], [103] and [004], at $2\theta = 34.42^{\circ}$, 36.25°, 62.86° and 72.56°. They are in good accordance with the JCPDS card No. 36-1451 with lattice constants of a = 3.25 Å and c = 5.21 Å. The sharp diffraction peak (002) indicates that the ZnO nanorods have grown along the *c*-axis. It were found a strong UV emission centered at 380 nm and a broad peak in the visible region 550 nm as shown in the inset[19]. In figure 2(b), HRTEM and SAED pattern images show the ZnO NRs is structurally uniform and contains no defects such as dislocations and stacking. It clearly shows the lattice spacing of 0.52 nm corresponds to *d*-spacing of (002) crystal planes, indicating the growth of the crystalline ZnO NRs along *c*-axis direction.

FE-SEM image with a 45^{o} tilt angle of the ZnO NR photodetectors is as shown in figure 3, the inset shows a 45^{o} tilt angle photograph of the NR arrays. The average length and diameter of these ZnO NRs were around 1-2 μm and ~100 nm, respectively. It was found that high density of well-aligned ZnO NR arrays were successfully grown on the gap of interdigitated electrodes.

Figure 4 shows current-voltage (*I-V*) characteristics of the fabricated traditional ZnO film and ZnO NR MSM PDs with the same Ag interdigitated electrodes measured in dark and under illumination. Photocurrent measurements were performed by the 370-nm. With 3 V applied bias, it was found that the dark current/ photocurrent were 96.4 nA/1.3 μA and 0.11 nA/19.6 μA for ZnO and ZnO NR MSM PDs, respectively. The photocurrent to dark current contrast ratios of the ZnO and ZnO NR PDs were 9.5×10^{2} and 3.23×10^{3}, respectively. The enhancement of UV light absorption could be attributed to the NR arrays having larger surface area than film in this investigation. Thus, the photocurrents generated from NR MSM PDs are increased much more than the traditional film MSM PDs.

The spectral responsivities of the ZnO MSM PDs with applied biases of 3 V are shown in figure 5. It can be seen that the photoresponsivities were nearly constants in the UV region (300-370 nm). We define the UV-to-visible rejection ratio as the responsivity measured at 360 nm divided by the responsivity at 450 nm. With such a definition and 3 V applied bias, we found the UV-to-visible rejection ratios are 88.46 and 282.59 for the ZnO film and ZnO NR MSM PDs, respectively. With an 370-nm illumination and 3 V bias, it was found that the responsivities for the fabricated ZnO film and ZnO NR PDs were 0.00236 and 0.0409 A/W, respectively. The responsivity of a detector, *R*, is defined as

$$R = \frac{I_{ph}}{P_{opt}} = \eta \frac{q\lambda}{hc} \ (\mathrm{A/W}),$$

where η is the external quantum efficiency, q is the electron charge, λ is the incident light wavelength, h is the Planck constant and c is the speed of light. By the expression, we found that the quantum efficiency of of 1.22 % and 0.07 % for the ZnO NR MSM PDs and ZnO film MSM PDs, respectively.

Table 1 summarizes photo/dark current, responsivities, UV-to-visible rejection ratios for ZnO NR and ZnO film MSM PDs. The ZnO NR MSM PDs show much higher photoresponse than the traditional ZnO MSM PDs can be attributed to the defects of NR surfaces which is the origin of the trap states, and the surrounding gas molecules completely affects energy band.[10, 11] It should be noted that the high density of trap states are usually found in NRs because of the dangling bonds at the surfaces. Furthermore, this leads to an increase of carrier injection and transport, producing a persistent photocurrent.

Conclusion

In summary, we have investigated the UV MSM PDs with selectively grown ZnO NR arrays. Compared with traditional ZnO MSM PD, the fabricated novel UV PD shows a higher photoresponse. With 3 V applied bias and 370 nm illumination on the NR devices, it was found that the photoresponsity and UV-to-visible rejection ratio are 0.0409 A/W and 282.59, respectively. On the other hand, the measured values of ZnO photodetectors with no NRs are 0.00236 A/W and 88.46, respectively. As a result, it can be attributed to high surface-to-volume ratio of the ZnO NRs and high density of trap states on the NRs. In other words, the very large surface-to-volume ratios of ZnO NR arrays easily promote oxygen adsorption and desorption at the NR surfaces. ZnO

NRs-based MSM PDs on flexible substrates is a most promising material for the production of the new generation of FEDs, and it has gained great commercial and scientific interest.

This work was supported by National Science Council of Taiwan under contract number NSC-95-2221-E-150-077-MY3 & NSC-95-2622-E-150-031-CC3.

References

1 L. W. Ji, Y. K. Su, S. J. Chang, S. H. Liu, C. K. Wang, S. T. Tsai, T. H. Fang, L. W. Wu, and Q. K. Xue, Solid-State Electron. **47**, 1753 (2003).

2 L. W. Ji, T. H. Fang, and T. H. Meen, Phys. Lett. A **355**, 118 (2006).

3 S. J. Young, L. W. Ji, S. J. Chang, and Y. K. Su, J. Cryst. Growth **293**, 43 (2006).

4 S. J. Young, L. W. Ji, S. J. Chang, Y. P. Chen, and S. M. Peng, Semicond. Sci. Technol. **23**, 085016 (2008).

5 L. W. Ji, S. J. Young, T. H. Fang, and C. H. Liu, Appl. Phys. Lett. **90**, 033109 (2007).

6 L. W. Ji, S. J. Chang, T. H. Fang, S. J. Young, and F. S. Juang, IEEE Trans. Nanotechnol. **7**, 1 (2008).

7 Y. Ryu, T. S. Lee, J. A. Lubguban, H. W. White, B. J. Kim, Y. S. Park, and C. J. Youn, Appl. Phys. Lett. **88**, 241108 (2006).

8 M. H. Huang, S. Mao, H. Feick, H. Q. Yan, Y. Y. Wu, H. Kind, E. Weber, R. Russo, and P. D. Yang, Science **292**, 1897 (2001).

9 H. Kind, H. Q. Yan, B. Messer, M. Law, and P. D. Yang, Adv. Mater. **14**, 158 (2002).

10 C. Soci, A. Zhang, B. Xiang, S. A. Dayeh, D. P. R. Aplin, J. Park, X. Y. Bao, Y. H. Lo, and D. Wang, Nano Lett. **7**, 1003 (2007).

11 Y. Z. Jin, J. P. Wang, B. Q. Sun, J. C. Blakesley, and N. C. Greenham, Nano Lett. **8**, 1649 (2008).

12 H. T. Ng, T. Yamada, P. Nguyen, Y. P. Chen, and M. Meyyappan, Nano Lett. **4**, 1247 (2004).

13 K. Keem, D. Y. Jeong, S. Kim, M. S. Lee, I. S. Yeo, U. I. Chung, and J. T. Moon, Nano Lett. **6**, 1454 (2006).

14 J. B. Baxter, and E. S. Aydil, Appl. Phys. Lett. **86**, 053114 (2005).

15 X. D. Wang, J. H. Song, J. Liu, and Z. L. Wang, Science **316**, 102 (2007).

16 Q. Wan, Q. H. Li, Y. J. Chen, T. H. Wang, X. L. He, J. P. Li, and C. L. Lin, Appl. Phys. Lett. **84**, 3654 (2004).

17 S. Logothetidis, Rev. Adv. Mater. Sci. **10**, 387 (2005).

18 A. Laskarakis, S. Logothetidis, J. Appl. Phys. **99,** 066101 (2006).

19 S. H. Jeong, B. S. Kim, and B. T. Lee, Appl. Phys. Lett. **82**, 2625 (2003)

TAB. 1. Photocurrent, dark current, photoresponsivity, and UV-to-visible rejection ratio of the ZnO MSM PDs measured at 3 V bias.

	Photo/ dark current	Responsivity (A/W)	UV-to-visible rejection ratio
ZnO NRs	0.606 nA/19.6 μA	0.0409	282.59
ZnO film	0.201 nA/1.91 μA	0.00236	88.46

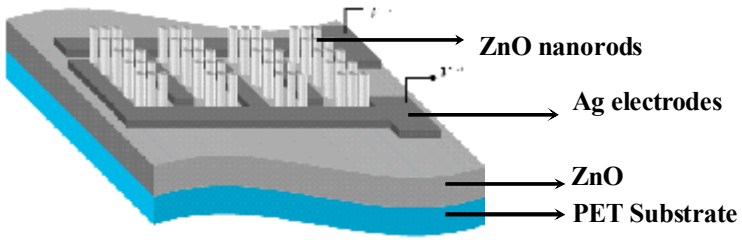

FIG. 1. Schematic for the fabricated UV MSM PDs with ZnO NR arrays.

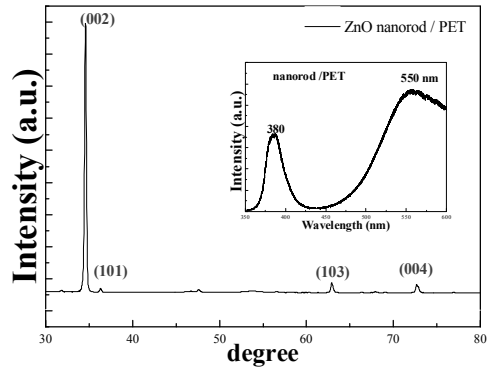

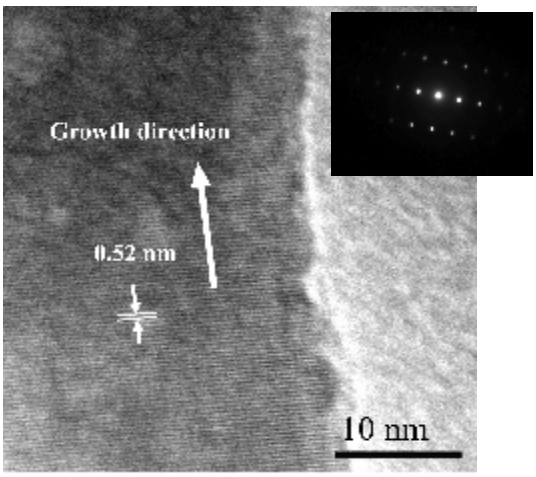

FIG. 2. (a) XRD result of ZnO NRs on ZnO/glass substrate. The inset shows room temperature PL spectrum of ZnO NRs. (b) HRTEM image of an individual ZnO NR, the lattice spacing is 0.52 nm along [002] direction, inset is the corresponding SAED image. (c) Raman spectrum of ZnO NR arrays.

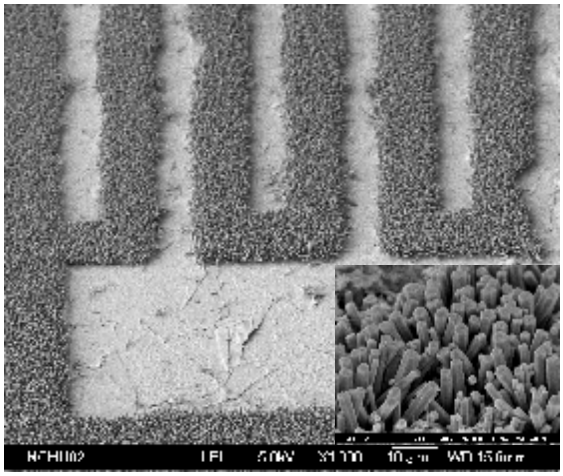

FIG. 3. FE-SEM image with 45° tilt angle for the ZnO NR MSM PDs. The inset shows the 45° tilt angle image of the ZnO NR arrays.

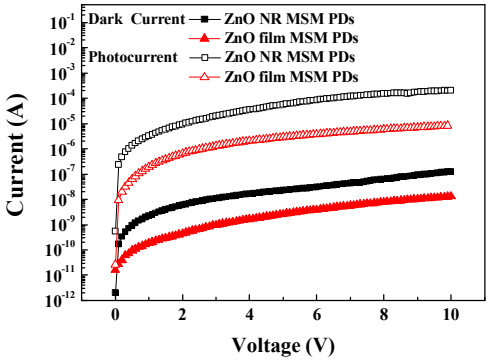

FIG. 4. I-V characteristics of the NR MSM PDs measured in dark and under 370-nm illumination.

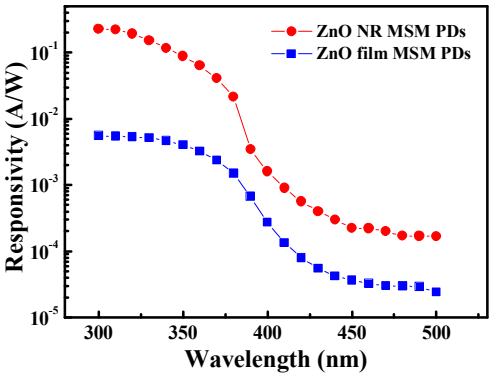

FIG. 5. Measured spectral reponsivities of the ZnO MSM PDs at 3 V applied bias.